Electronic spectrum of UO2(2+) and [UO2Cl4]2- calculated with time-dependent density functional theory

Pierloot, K.; van Besien, E.; van Lenthe, E.; Baerends, E.J.

published in
Journal of Chemical Physics
2007

DOI (link to publisher)
10.1063/1.2735297

document version
Publisher's PDF, also known as Version of record

Electronic spectrum of UO_2^{2+} and $[UO_2Cl_4]^{2-}$ calculated with time-dependent density functional theory

Kristine Pierloot[a] and Els van Besien
Department of Chemistry, University of Leuven, Celestijnenlaan 200F, B-3001 Heverlee-Leuven, Belgium

Erik van Lenthe and Evert Jan Baerends
Theoretical Chemistry, Vrije Universiteit, De Boelelaan 1083, NL-1081 HV Amsterdam, The Netherlands

(Received 14 February 2007; accepted 4 April 2007; published online 17 May 2007)

The electronic spectra of UO_2^{2+} and $[UO_2Cl_4]^{2-}$ are calculated with a recently proposed relativistic time-dependent density functional theory method based on the two-component zeroth-order regular approximation for the inclusion of spin-orbit coupling and a noncollinear exchange-correlation functional. All excitations out of the bonding σ_u^+ orbital into the nonbonding δ_u or ϕ_u orbitals for UO_2^{2+} and the corresponding excitations for $[UO_2Cl_4]^{2-}$ are considered. Scalar relativistic vertical excitation energies are compared to values from previous calculations with the CASPT2 method. Two-component adiabatic excitation energies, U–O equilibrium distances, and symmetric stretching frequencies are compared to CASPT2 and combined configuration-interaction and spin-orbit coupling results, as well as to experimental data. The composition of the excited states in terms of the spin-orbit free states is analyzed. The results point to a significant effect of the chlorine ligands on the electronic spectrum, thereby confirming the CASPT2 results: The excitation energies are shifted and a different luminescent state is found. © *2007 American Institute of Physics*.
[DOI: 10.1063/1.2735297]

I. INTRODUCTION

Mainly because of the relatively low computational cost, time-dependent density functional theory[1,2] (TDDFT) has nowadays become one of the most popular methods for the calculation of electronic spectra. For systems containing heavy elements, relativistic effects play an important role in the electronic structure.[3] Until recently, only scalar relativistic effects could be taken into account in TDDFT calculations, while spin-orbit coupling (SOC) effects were neglected. Exceptions are the work of Toffoli *et al.*[4] on mercury and Gao *et al.*[5] on rare gas and Group XII atoms. Recently, Wang *et al.*[6] proposed a relativistic TDDFT formalism that makes use of the two-component zeroth-order regular approximation[7–11] (ZORA) and the noncollinear exchange-correlation (XC) potential.[12–14] Compared to other TDDFT formalisms that can also deal with SOC,[4,5] this formalism has a correct nonrelativistic limit and recovers the threefold degeneracy of triplet excitations for closed-shell systems. This two-component relativistic TDDFT formalism has been implemented in the Amsterdam density functional (ADF) program,[15–17] with full use of double group symmetry. Applications to the excitation energies of some closed-shell atoms, ions, diatomic molecules, as well as transition metal complexes containing heavy elements have shown promising results, with an error comparable to nonrelativistic TDDFT calculations on light elements.[6,18]

In the present work, the two-component relativistic TDDFT formalism proposed by Wang *et al.*[6] has been used to calculate the electronic spectrum of UO_2^{2+} and $[UO_2Cl_4]^{2-}$. For the first time, an application of relativistic TDDFT on compounds containing an element heavier than a transition metal is reported. The electronic spectrum of uranyl and its complexes has fascinated scientists already for ages. Uranyl is by far the most well known of all actinyl ions and its absorption and luminescence spectrum have extensively been studied experimentally. The typical spectral structure of uranyl complexes between 20 000 and 30 000 cm^{-1} originates from transitions out of the highest-lying bonding σ_u^+ orbitals, with strongly mixed uranium and oxygen character, into the lowest nonbonding δ_u or ϕ_u orbitals, both almost pure U5*f*. The high energy of the σ_u^+ orbital relative to the other three bonding combinations of π_u, σ_g^+, and π_g symmetries has been explained[19–23] by a "pushing from below" mechanism involving the pseudocore U6p_σ orbital, i.e., a destabilization of σ_u^+ as the result of antibonding admixture of U6*p* into the otherwise bonding U5*f*/O2*p* combination.

Detailed spectroscopic studies have been reported by Denning and co-workers on crystalline $CsUO_2Cl_4$ and $CsUO_2(NO_3)_3$.[24,25] Electronic spectra of uranyl with a manifold of different ligands, mainly in solution, have been studied by Görller-Walrand and Vanquickenborne.[26,27] The experimental data indicate that the energy of the low-lying excited states is relatively independent of the nature of the equatorial ligands. The first detailed *ab initio* calculations[28,29] were performed using a combined configuration-interaction (CI) and spin-orbit coupling method, denoted as SOC-CI. A comparison of the calculated spectra of free, uncomplexed uranyl ion with the complex $[UO_2Cl_4]^{2-}$ showed only a small shift of the excitation energies (at most 2000 cm^{-1}) and no change in the character of

[a]Author to whom correspondence should be addressed. Fax: +32 16 32 79 92; Electronic mail: kristin.pierloot@chem.kuleuven.be

the low-lying excited states. From this it was concluded that the spectrum is not only independent of the type of equatorial ligands but even of the mere presence of an equatorial ligand field. However, a different conclusion was drawn from more recent calculations[30] performed with the CASPT2 method (second-order perturbation theory based on a complete-active-space reference wave function) on UO_2^{2+} and $[UO_2Cl_4]^{2-}$. These calculations indicated a considerable blueshift (by 1500–4300 cm^{-1}) of the energies by the presence of the chlorine ligands. Furthermore, a change in the character of the luminescent state between both molecules was found, from Δ_g (predominantly $\sigma_u^+ \rightarrow \phi_u$) in UO_2^{2+} to Π_g (predominantly $\sigma_u^+ \rightarrow \delta_u$) in $[UO_2Cl_4]^{2-}$. The accuracy of the latter method was proven by the very close correspondence between the CASPT2 excitation energies and the available experimental data for $[UO_2Cl_4]^{2-}$.

In this work, both vertical and adiabatic excitation energies are reported for UO_2^{2+} and $[UO_2Cl_4]^{2-}$, calculated with TDDFT, both without and with inclusion of SOC. The performance of different functionals is compared. U–O equilibrium distances and symmetric stretching frequencies have been calculated with SOC and compared to experiment and to previous computational results. For UO_2^{2+}, all excitations out of the bonding σ_u^+ orbitals into the nonbonding δ_u or ϕ_u orbitals have been analyzed in detail. For $[UO_2Cl_4]^{2-}$, these correspond to transitions out of a_{2u} into b_{1u}, b_{2u}, and e_u.

II. COMPUTATIONAL DETAILS

All excitation energies were calculated with the time-dependent density functional theory as implemented in the ADF program package.[15,16] For the XC potential, several functionals were used: LDA,[31] BP86,[32,33] LB94,[34] and SAOP.[35] The latter two functionals were especially designed for the calculation of response properties. For the exchange-correlation kernel the adiabatic local-density approximation has been used throughout.

In calculations containing heavy elements, such as uranium, relativistic effects play an important role. Scalar relativistic effects were included via the ZORA formalism.[7–11] These results will be referred to as spin-orbit free or SOF. A two-component ZORA TDDFT formalism was used for the inclusion of SOC effects. The usual linear response approach of TDDFT is followed, where now the Hamiltonian includes the spin-orbit coupling terms. It is a special feature of our implementation that the noncollinear approach is followed in the calculation of the exchange-correlation functionals. This also has the effect that a correct nonrelativistic limit is obtained, in the sense that, for closed-shell ground state systems, it recovers the correct threefold degeneracy of excitations to triplet states. More details of this method can be found in Ref. 6. The SOF *fragment* used in the calculation with SOC was obtained with the PW91 functional.[36] All calculations were performed using QZ4Pae basis sets (quadruple-ζ all electron basis sets with four polarization functions) of Slater-type orbitals, optimized for the use in the ZORA equation.[37] The ADF numerical integration parameter was set to 6.0 in all calculations. The full symmetry of the compounds was used, i.e., $D_{\infty h}$ for UO_2^{2+} and D_{4h} for $[UO_2Cl_4]^{2-}$.

TABLE I. Resolution of the relevant symmetry species of $D_{\infty h}$ into the species of D_{4h}.

$D_{\infty h}$	D_{4h}
σ_g^+	a_{1g}
σ_u^+	a_{2u}
π_g	e_g
π_u	e_u
δ_g	$b_{1g}+b_{2g}$
δ_u	$b_{1u}+b_{2u}$
ϕ_g	e_g
ϕ_u	e_u
γ_g	$a_{1g}+a_{2g}$
γ_u	$a_{1u}+a_{2u}$

In the calculations for UO_2^{2+} all possible single excitations out of the highest occupied bonding orbital σ_u^+ into the nonbonding orbitals δ_u and ϕ_u were considered, giving rise to the SOF excited states $^3\Delta_g$, $^3\Phi_g$, $^1\Phi_g$, and $^1\Delta_g$. For $UO_2Cl_4^{2-}$, this corresponds to excitations out of a_{2u} into b_{1u}, b_{2u}, and e_u, resulting in $^3B_{1g}$, $^3B_{2g}$, ^3E_g, ^1E_g, $^1B_{1g}$, and $^1B_{2g}$. The correlation between the symmetry types in $D_{\infty h}$ and in D_{4h} can be found in Table I. Note that the complexes are oriented such that the z axis coincides with the uranyl axis and, for $UO_2Cl_4^{2-}$, the chloride ions are located between the x and y axes. Also note that for UO_2^{2+} we have chosen to maintain the $D_{\infty h}$ single-group notation $(\Sigma, \Pi, \Delta, \ldots)$ also after including SOC, instead of switching to the alternative double-group Ω notation. Although the latter notation has become more popular among quantum chemists[28,29] the former notation is used most frequently in experimental work,[24] and was also used by us in our previous work.[30]

In order to allow a direct comparison to the available CASPT2 results,[30] the same geometry was used for the calculation of the vertical spectra. The distance between the central uranium and the oxygen atom is 1.708 Å in UO_2^{2+} and 1.783 Å in $UO_2Cl_4^{2-}$. The distance between the uranium atom and the chlorine ligands in $UO_2Cl_4^{2-}$ is 2.712 Å. To obtain the optimal U–O bond lengths $[R_e(U-O)]$, adiabatic excitation energies (T_e), and symmetric harmonic U–O stretching frequencies (ω_e) for each state, calculations were performed at U–O distances ranging from 1.650 to 1.850 Å for UO_2^{2+} and from 1.700 to 1.900 Å for $[UO_2Cl_4]^{2-}$, with intervals of 0.01 Å. Excited state energies were obtained by adding SAOP excitation energies to BP86 ground state energies. The desired properties were obtained from a quadratic fit of these energies versus the U–O bond length.

III. RESULTS AND DISCUSSION

A. Results without spin-orbit coupling

Vertical excitation energies calculated with TDDFT are presented in Table II for UO_2^{2+} and in Table III for $[UO_2Cl_4]^{2-}$. Energies obtained from previous CASTP2 calculations are given for comparison.[30] The absolute excitation energies strongly depend on the applied functional. Similar results are obtained with LDA and BP86. However, as com-

TABLE II. SOF vertical excitation energies of UO_2^{2+} calculated with TD-DFT and different functionals and with CASPT2.

$D_{\infty h}$	LDA	BP86	LB94	SAOP	CASPT2[a]
$^3\Phi_g$	15 582	15 440	10 773	24 147	22 922
$^3\Delta_g$	18 480	18 735	13 927	25 884	22 476
$^1\Phi_g$	19 132	19 008	14 412	27 675	27 194
$^1\Delta_g$	24 148	24 352	19 409	31 698	30 308

[a]Reference 30.

pared to CASPT2, these results are far too low. Such large deviations are conform with previous TDDFT studies on metal complexes, where the common functionals gave unsatisfying results as well.[38] Generally, the results can be greatly improved by the use of so-called *shape-corrected* potentials or model potentials, such as LB94 and the more recent SAOP. However, in this case the energies computed with the LB94 functional are even worse than with LDA or BP86. Clearly, this functional cannot be trusted for excited state calculations on uranyl and uranyl complexes. For both molecules, the energies obtained with the SAOP functional most closely agree with the CASPT2 results. For UO_2^{2+}, all SAOP energies are higher than the CASPT2 values, with differences ranging between 481 cm^{-1} for $^1\Phi_g$ and 3408 cm^{-1} for $^3\Delta_g$. On the other hand, For $[UO_2Cl_4]^{2-}$, all SAOP excitation energies are lower than the CASPT2 energies. Apart from the two lowest excited states $^3B_{1g}$ and $^3B_{2g}$, the differences between SAOP and CASPT2 are also considerably larger for $[UO_2Cl_4]^{2-}$ than for UO_2^{2+}. This is particularly true for the three singlet states, with a maximum deviation of 6136 cm^{-1} for the $^1B_{2g}$ state.

An important difference between the CASPT2 and DFT results concerns the splitting between the triplet and singlet state belonging to the same configuration. With CASPT2, these splittings are similar for both molecules, 3400–4200 cm^{-1} for the $^{3,1}\Phi_g(\sigma_u^+ \rightarrow \phi_u)$ states and 7800–7900 cm^{-1} for the $^{3,1}\Delta_g(\sigma_u^+ \rightarrow \delta_u)$ states. With DFT, much smaller singlet-triplet splittings are obtained. Furthermore, the reduction (as compared to CASPT2) is considerably larger for $[UO_2Cl_4]^{2-}$ than for UO_2^{2+}. With SAOP, the calculated splittings are only 1122 cm^{-1} for the E_g states in $[UO_2Cl_4]^{2-}$, as compared to 3528 cm^{-1} for Φ_g in UO_2^{2+}, and 2000–2330 cm^{-1} for the B_{1g} and B_{2g} states in $[UO_2Cl_4]^{2-}$, as compared to 5814 cm^{-1} for Δ_g in UO_2^{2+}.

Comparing the excitation energies obtained with the same method for both molecules, we note that while CASPT2 predicts a significant blueshift of the spectrum of $[UO_2Cl_4]^{2-}$ as compared to UO_2^{2+}, the SAOP results show the opposite trend: with exception of the $^3\Phi_g$ state (^3E_g in $[UO_2Cl_4]^{2-}$), all excitation energies are lowered by 2000–7000 cm^{-1} by the addition of chlorines in the equatorial field of uranyl. The blueshift of the bands in the CASPT2 spectrum is larger for the $^{3,1}\Phi_g(\sigma_u^+ \rightarrow \phi_u)$ states than for the $^{3,1}\Delta_g(\sigma_u^+ \rightarrow \delta_u)$ states. In Ref. 30 this was explained by noting that from the two nonbonding orbitals δ_u and ϕ_u in UO_2^{2+}, the ϕ_u orbital is raised in energy relative to δ_u in $[UO_2Cl_4]^{2-}$, due to (mainly electrostatic) σ interaction between this orbital and the equatorial chlorine σ orbitals of the same symmetry. This effect is obviously not confirmed by the DFT results.

TABLE III. SOF vertical excitation energies $[UO_2Cl_4]^{2-}$ calculated with TDDFT and different functionals and with CASPT2.

D_{4h}	LDA	BP86	LB94	SAOP	CASPT2[a]
$^3B_{1g}$	18 302	18 539	13 408	22 601	22 862
$^3B_{2g}$	19 246	19 489	14 670	23 825	23 711
^3E_g	20 251	20 288	16 556	24 715	27 175
$^1B_{1g}$	21 051	21 301	15 041	24 600	30 736
^1E_g	21 756	21 805	17 102	25 837	30 624
$^1B_{2g}$	22 315	22 535	16 925	26 153	31 578

[a]Reference 30.

The different energetic effects of the equatorial chlorine ligand field observed at the CASPT2 and DFT levels may be brought back to the different compositions of the orbitals involved. In UO_2^{2+}, both methods essentially give the same orbital composition. The accepting orbitals δ_u and ϕ_u are in this case of course pure Uf (there is no oxygen partner of the same symmetry), while the departing orbital σ_u^+ in both cases contains an almost equally composed mixture of Uf (55%–56%), Up (9%–10%), and Op (33%–34%) character. In $[UO_2Cl_4]^{2-}$, both methods predict a limited admixture of chlorine character in the accepting orbitals e_u and b_{1u} (b_{2u} still with no ligand partner, therefore remaining pure Uf), with DFT predicting a larger contribution (8% for e_u, 5% for b_{1u}) than CASPT2 (2% for e_u, 1% for b_{1u}). However, a much more important difference between both methods is found for the departing a_u orbital. With CASPT2, this orbital remains almost completely localized on the uranyl moiety (44% Uf, 43% Op, 12% Up), with only 1% chlorine character. However, the DFT results show a completely different picture, with the a_u orbital now attaining a dominant (73%) chlorine contribution, with the remaining 27% divided almost equally between uranium (11% Uf, 3% Up) and oxygen (13%). Such an unrealistically high chlorine character of the highest occupied molecular orbital (HOMO) would point to a very covalent uranyl-chlorine interaction in $[UO_2Cl_4]^{2-}$, which is obviously not confirmed by CASPT2 or by the experimental spectroscopic data.[24] A similar problem was observed in a recent DFT study of the bonding and spectroscopic properties of the $[CuCl_4]^{2-}$ complex.[39] Also there, DFT (both BP86 an B3LYP) were found to predict a too covalent Cu–Cl description, giving rise to an underestimation of the (ligand-to-metal) charge-transfer excitations energies in this complex. Also in $[UO_2Cl_4]^{2-}$ the redshift of the TDDFT spectrum as compared to UO_2^{2+} as well as to the CASPT2 results for the same complex may be explained by an incorrect composition and concomitant too high energy of the a_u orbital. Furthermore, the high chlorine content of the latter orbitals also gives the lowest excited states in the SAOP-DFT spectrum of $[UO_2Cl_4]^{2-}$ much more charge-transfer character than their CASPT2 analogs. This may explain the much smaller singlet-triplet splittings observed with the former method.

B. Results with spin-orbit coupling

In Table IV, SAOP vertical excitation energies for UO_2^{2+} including SOC are given for all states corresponding to the

TABLE IV. Vertical excitation energies of UO_2^{2+} calculated with SOC, and composition of the excited states in terms of the SOF $\sigma_u^+ \rightarrow \delta_u, \phi_u$ states.

	SAOP-TDDFT					CASPT2[a]				
		Composition (%)					Composition (%)			
		$\sigma_u^+ \rightarrow \delta_u$		$\sigma_u^+ \rightarrow \phi_u$			$\sigma_u^+ \rightarrow \delta_u$		$\sigma_u^+ \rightarrow \phi_u$	
$D_{\infty h}$	ΔE (cm–1)	$^3\Delta_g$	$^1\Delta_g$	$^3\Phi_g$	$^1\Phi_g$	ΔE (cm^{-1})	$^3\Delta_g$	$^1\Delta_g$	$^3\Phi_g$	$^1\Phi_g$
$a\,\Delta_g$	20 345	7	3	87		19 195	23	2	74	
$a\,\Phi_g$	21 431	11		60	23	20 265	27		51	18
$a\,\Pi_g$	23 784	94				20 104	97			
$b\,\Delta_g$	25 430	77	12	3		22 230	69	9	19	
$a\,\Gamma_g$	27 069			95		26 312			97	
$b\,\Phi_g$	28 465	48		30	15	25 435	67		29	1
$c\,\Phi_g$	29 424	36		5	49	29 085	3		17	74
$c\,\Delta_g$	32 018	7	56	9		31 314	4	79	6	

[a]Reference 30.

SOF states in Table II. The contribution of the different SOF states to each excited state is also included. For all but the highest $c\,\Delta_g$ state these contributions add up to 90% or more, thus pointing to the absence of considerable mixing with higher-lying SOF states. As illustrated further (Fig. 1), the lowest excitations out of the highest π_u-type bonding orbital (not included in Table IV), in fact, already appear at slightly lower energies than the highest $\sigma_u^+ \rightarrow \delta_u, \phi_u$ state $c\,\Delta_g$, thus explaining the larger multiconfigurational character found for this state.

Overall, the agreement between the DFT and CASPT2 results in Table IV is satisfactory. All DFT results are somewhat higher than the CASPT2 values, with differences ranging between 339 and 3680 cm^{-1}. Looking at the composition of the different states, these differences can be brought back to the SOF data in Table II. The largest differences are found

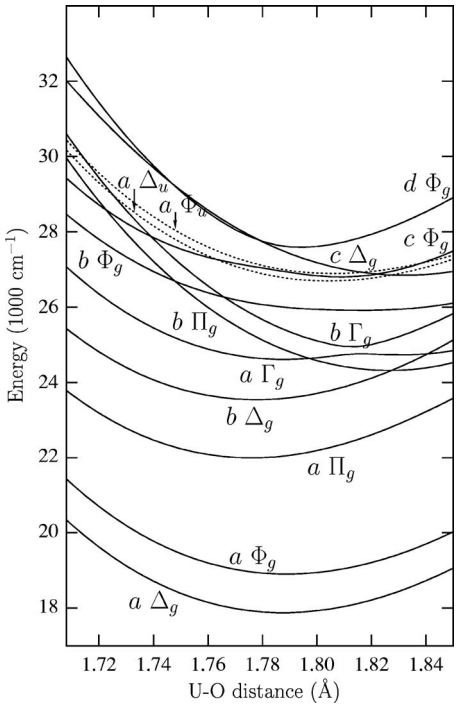

FIG. 1. Excited state curves of UO_2^{2+} along the U–O symmetric stretching path obtained from SAOP-TDDFT calculations.

for the states with predominant $^3\Delta_g$ character $a\,\Pi_g$ (3680 cm^{-1}), $b\,\Delta_g$ (3110 cm^{-1}), and $b\,\Phi_g$ (3030 cm^{-1}), close to the difference of 3408 cm^{-1} found for the parent $^3\Delta_g$ state in Table II. For the $a\,\Delta_g$, $b\,\Phi_g$, and $a\,\Gamma_g$ states, the differences are smaller, 757–1166 cm^{-1}, conforming with the difference of 1225 cm^{-1} obtained for their parent $^3\Phi_g$ state. For the two highest states with predominant singlet character, $c\,\Phi_g$ and $c\,\Delta_g$, the SAOP and CASPT2 results are very close (within 1000 cm^{-1}), as was the case for the corresponding singlet states in Table II. The smaller singlet-triplet splittings of the SOF states observed from DFT as compared to CASPT2 are also reflected in the composition of the SOC states in Table IV, showing more extensive mixing of singlet and triplet characters in the DFT results.

Table V presents the vertical excitation energies calculated with SOC for $[UO_2Cl_4]^{2-}$. To simplify the comparison with the results for UO_2^{2+}, each D_{4h} state is also given its $D_{\infty h}$ parentage. Conforming with the SOF results in Table III, all SAOP energies in Table V remain lower than the corresponding CASPT2 energies also after including SOC, with differences increasing with increasing excitation energy. For the lowest excited states $a\,\Pi_g$, $a\,\Delta_g$, and $a\,\Phi_g$ both methods agree to within 1000 cm^{-1}, whereas for the highest states $c\,\Delta_g$ and $c\,\Phi_g$ the difference amounts to 3600–4300 cm^{-1}. As for UO_2^{2+}, the smaller singlet-triplet splittings obtained from SAOP as compared to CASPT2 give rise to much more extensive mixing of singlet and triplet characters when introducing SOC in the former method. Whereas in the CASPT2 results in Table V one can still recognize a lower-lying triplet block below 30 000 cm^{-1} and a higher-lying singlet block starting at 32 000 cm^{-1}, both spin multiplicities are more thoroughly mixed at the SAOP level, with the two highest states $c\,\Delta_g$ and $c\,\Phi_g$ retaining 50% or less singlet character. Furthermore, also within the triplet block more extensive mixing is found with SAOP between states belonging to either $^3\Delta_g$ or $^3\Phi_g$. This can again be traced back to the SOF results in Table V, where both states are well separated at the CASPT2 level but close in energy at the SAOP level. As a result, the lowest excited states in the CASPT2 spectrum of $[UO_2Cl_4]^{2-}$ are predominantly $^3\Delta_g$, while the lowest state obtained from SAOP, $a\,B_{2g}$, is an almost equal mixture of

TABLE V. Vertical excitation energies of $[UO_2Cl_4]^{2-}$ calculated with SOC, and composition of the excited states in terms of the SOF $\sigma_u^+ \rightarrow \delta_u, \phi_u$ states.

		SAOP-TDDFT							CASPT2[a]						
			Composition (%)							Composition (%)						
			$\sigma_u^+ \rightarrow \delta_u$				$\sigma_u^+ \rightarrow \phi_u$			$\sigma_u^+ \rightarrow \delta_u$				$\sigma_u^+ \rightarrow \phi_u$	
D_{4h}	$D_{\infty h}$	ΔE (cm^{-1})	$^3B_{2g}$	$^3B_{1g}$	$^1B_{2g}$	$^1B_{1g}$	^3E_g	^1E_g	ΔE (cm^{-1})	$^3B_{2g}$	$^3B_{1g}$	$^1B_{2g}$	$^1B_{1g}$	^3E_g	^1E_g
$a\,B_{2g}$	$a\,\Delta_g$	20 884		44	1		46		21 273		67			31	
$a\,E_g$	$a\,\Pi_g$	20 954	13	60			9	1	21 024	28	66			2	1
$a\,B_{1g}$	$a\,\Delta_g$	21 335	8			9	74		22 125	53				44	
$b\,E_g$	$a\,\Phi_g$	22 108	36	1			31	20	22 859	43	8			32	15
$b\,B_{1g}$	$b\,\Delta_g$	22 420	54			34			24 056	38			16	44	
$b\,B_{2g}$	$b\,\Delta_g$	22 570		30	29		32		24 339		26	12		60	
$c\,E_g$	$b\,\Phi_g$	26 882	36	26			13	7	27 494	26	23			42	7
$a\,A_{2g}$	$a\,\Gamma_g$	27 678					89		29 842					97	
$a\,A_{1g}$	$a\,\Gamma_g$	27 682					85		29 849					97	
$c\,B_{1g}$	$c\,\Delta_g$	27 666	20			46	18		31 991	7			76	10	
$d\,E_g$	$c\,\Phi_g$	28 364		1			32	50	31 961	1	1			22	72
$c\,B_{2g}$	$c\,\Delta_g$	28 561		16	17		7		32 523		5	81		8	

[a]Reference 30.

$^3\Delta_g$ and $^3\Phi_g$. We also note that the order of the lowest two excited states, $a\,B_{2g}$ and $a\,E_g$, is interchanged with SAOP as compared to CASPT2. Considering the average of the $a\,B_{2g}$ and $a\,B_{1g}$ both methods, however, predict the same ordering of the lowest excited states in $[UO_2Cl_4]^{2-}$: $a\,\Pi_g < a\,\Delta_g < a\,\Phi_g$.

Concerning the composition of the excited states in Table V we further note that the total of all contributions adds up to 82% or more for all states except the highest $c\,B_{2g}$ state. This means that, although SOC introduces more significant interconfigurational mixing than in UO_2^{2+} with SOF states belonging to other higher-lying excitations, the lowest states in the spectrum of $[UO_2Cl_4]^{2-}$ still essentially correspond to excitations out of the HOMO σ_u^+ orbital. We should note, however, that the lowest $\pi_u \rightarrow \delta_u, \phi_u$ states are in fact predicted by SAOP-TDDFT to appear at 23 000–26 000 cm^{-1} in the vertical spectrum of $[UO_2Cl_4]^{2-}$, i.e., between the $b\,B_{2g}$ and $c\,E_g$ states. At the CASPT2 level, the onset of these states is located more than 10 000 cm^{-1} higher in energy, namely, at 35 760 cm^{-1}.[30] Analysis of the experimental data[24,25] also shows no indication of low-lying states corresponding to an excitation out of π_u. We therefore decided not to give these states any further attention, thus not including them in Table V.

For a detailed comparison with experimental electronic energy levels, adiabatic excitation energies should be considered. They are presented in Table VI for UO_2^{2+} and in Table VII for $[UO_2Cl_4]^{2-}$, along with the optimal U–O distances R(U–O) and harmonic frequencies ω_e of the symmetric U–O stretching vibration of the different states. Only the lowest excited states have been included in both tables. For the higher states, forbidden crossings occur at increasing U–O distances between the higher-lying states corresponding to an excitation from σ_u^+ and the lowest states corresponding to an excitation out of the highest π_u bonding orbitals, thus preventing a quadratic analysis of the excited state energy curves involved. This is illustrated in Fig. 1 for UO_2^{2+}, showing all lowest excited state curves obtained from SAOP along the U–O symmetric stretching path. A similar plot obtained from CASPT2 may be found in Ref. 30. At the ground state structure (the origin of the x axis in Fig. 1), the spectral region below 30 000 cm^{-1} is indeed built from states with almost exclusive $\sigma_u^+ \rightarrow \delta_u, \phi_u$ character. Only the highest $c\,\Delta_g$ state included in Table IV is in fact located amongst the lowest $\pi_u \rightarrow \delta_u, \phi_u$ states, $b\,\Pi_g$ (29 963 cm^{-1}), $b\,\Gamma_g$ (30 603 cm^{-1}), $d\,\Phi_g$ (32 643 cm^{-1}). The latter states, however, descent much more steeply with increasing U–O dis-

TABLE VI. Adibatic spectrum of UO_2^{2+} with SOC.

	SAOP-TDDFT			CASPT2[a]			SOC-CI[b]		
$D_{\infty h}$	R_e(U-O) (Å)	ω_e (cm^{-1})	T_e (cm^{-1})	R_e(U-O) (Å)	ω_e (cm^{-1})	T_e (cm^{-1})	R_e(U-O) (Å)	ω_e (cm^{-1})	T_e (cm^{-1})
$X\,\Sigma_g^+$	1.716	984		1.708	974		1.668	1103	
$a\,\Delta_g$	1.788	847	**17 909**	1.782	815	**17 227**	1.739	845	21 421
$a\,\Phi_g$	1.789	847	18 933	1.783	811	18 239	1.742	847	22 628
$a\,\Pi_g$	1.776	854	22 022	1.765	847	18 888	1.733	867	**20 719**
$b\,\Delta_g$	1.778	854	23 569	1.769	844	20 911	1.749	900	23 902
$a\,\Gamma_g$	1.788	822	24 637	1.784	808	24 190	1.755	880	27 893

[a]Reference 30.
[b]Reference 29.

TABLE VII. Adiabatic spectrum of $[UO_2Cl_4]^{2-}$ with SOC.

		SAOP-TDDFT			CASPT2[a]			SOC-CI[b]			Expt.[c]	
D_{4h}	$D_{\infty h}$	R_e(U-O) (Å)	ω_e (cm^{-1})	T_e (cm^{-1})	R_e(U-O) (Å)	ω_e (cm^{-1})	T_e (cm^{-1})	R_e(U-O) (Å)	ω_e (cm^{-1})	T_e (cm^{-1})	ω_e (cm^{-1})	T_e (cm^{-1})
$X\,A_{1g}$	$X\,\Sigma_g^+$	1.808	803		1.783	819		1.728	968		832	
$a\,E_g$	$a\,\Pi_g$	1.845	733	20 059	1.836	712	**20 280**	1.790	885	**20 363**	715	**20 096**
$a\,B_{2g}$	$a\,\Delta_g$	1.847	732	**19 908**	1.844	703	20 330	1.792	879	21 013	710	20 407
$a\,B_{1g}$	$a\,\Delta_g$	1.848	739	20 308	1.846	698	21 139	1.790	878	21 838	696	21 316
$b\,E_g$	$a\,\Phi_g$	1.845	739	21 088	1.846	711	21 809	1.794	874	22 819	711	22 051
$b\,B_{1g}$	$b\,\Delta_g$	1.842	741	21 605	1.846	721	22 984	1.806	902	21 618	717	22 406
$b\,B_{2g}$	$b\,\Delta_g$	1.844	740	21 693	1.847	714	23 228	1.806	900	24 780	711	22 750

[a]Reference 30.
[b]Reference 29.
[c]Reference 24 and 25.

tance, leading to mixing and forbidden crossings with the $\sigma_u^+ \rightarrow \delta_u, \phi_u$ states. Similar crossings were also found from the CASPT2 calculations in Ref. 30. However, at the CASPT2 level the onset of the $\pi_u \rightarrow \delta_u, \phi_u$ states is located about 3000 cm^{-1} higher in energy than at the SAOP level, such that these crossings occur at larger U–O distances, behind the minima of the lowest excited state curves. As already mentioned, for $[UO_2Cl_4]^{2-}$ a number of $\pi_u \rightarrow \delta_u, \phi_u$ states are already found in the region between 23 000 and 26 000 cm^{-1} in the SAOP vertical spectrum, thus preventing a quadratic analysis for the higher-lying states in Table V.

For the free uranyl ion, no experimental spectral data are available. The SAOP results in Table VI can therefore only be compared to previous theoretical results obtained by either CASPT2 (Ref. 30) or SOC-CI.[28,29] On the other hand, for $[UO_2Cl_4]^{2-}$ Table VII also includes the experimental data obtained from the detailed experimental analysis of Denning and co-workers of the solid state spectrum of $Cs_2UO_4Cl_4$.[24,25]

Looking first at the U–O distances and frequencies we note the following trends. Considering the excited states, all three methods predict a weakening of the U–O bonds as compared to the ground state, due to the excitation of an electron from a bonding into a nonbonding orbital. This is reflected by a calculated increase of the U–O bond distances by 0.07–0.09 Å in UO_2^{2+} and 0.03–0.08 Å in $[UO_2Cl_4]^{2-}$, and by a decrease of the stretching frequencies by 140–260 cm^{-1} in UO_2^{2+} and 60–120 cm^{-1} in $[UO_2Cl_4]^{2-}$. The latter is also confirmed by the experimental symmetric U–O stretching frequencies in $Cs_2UO_4Cl_4$, showing a similar decrease with, on the average, 122 cm^{-1}. As compared to the experimental frequencies for $[UO_2Cl_4]^{2-}$, the results obtained with CASPT2 are closest, with the largest deviation, 13 cm^{-1}, found for the ground state. Slightly larger deviations, ranging between 18 and 43 cm^{-1}, are obtained with SAOP-TDDFT. However, the TDDFT results are obviously superior to the SOC-CI results, predicting frequencies that are systematically too high by 130–189 cm^{-1}. Similar trends are found for UO_2^{2+}. Here, the DFT frequencies are slightly (up to 36 cm^{-1}) larger than the CASPT2 results. For the lowest excited states the TDFFT and SOC-CI results are similar, whereas for the ground state and the higher excited states the SOC-CI results are again much higher (up to 120 cm^{-1}). The fact that SOC-CI overestimates the U–O bond strength is also reflected by the U–O distances obtained from this method, which are systematically shorter by 0.02–0.08 Å in both molecules than the DFT or CASPT2 results. The distances obtained from the latter two methods are close. The largest difference, 0.025 Å, is found for the ground state in $[UO_2Cl_4]^{2-}$, whereas for all other states the differences are of the order of 0.01 Å or less. It is also worth mentioning that, conforming with CASPT2,[30] the effect of SOC on the ground state DFT structure is found to be insignificantly small for both molecules. For a more detailed discussion of available ground state structural data in the literature we would like to refer to our previous work.[30,40]

For $[UO_2Cl_4]^{2-}$ excellent agreement is found between the DFT excitation energies and the experimental data. All energies are slightly too low, but the error never exceeds 1000 cm^{-1}, and are even smaller for the lowest two excited states: 37–500 cm^{-1}. A slightly closer agreement, 500 cm^{-1}, is, on the average, obtained at the CASPT2 level. However, also for the excitation energies in $[UO_2Cl_4]^{2-}$ the present SAOP-DFT results are superior to the SOC-CI results, which are all systematically too high by up to more than 2000 cm^{-1}. Given the close agreement between the CASPT2 excitation energies and the experimental data for $[UO_2Cl_4]^{2-}$, we consider the CASPT2 results as benchmark values for UO_2^{2+}, for which no experimental data are available. Also for this molecule, the SAOP energies are systematically closer to the CASPT2 results than the SOC-CI energies, the latter being too high by up to 4000 cm^{-1}. The deviations obtained with DFT show the same trend as was already discussed for the vertical excitation energies in Table IV, and brought back there to the SOF SAOP-DFT results in Table II. Indeed, for the three states $a\,\Delta_g$, $a\,\Phi_g$, and $a\,\Gamma_g$ with predominant $^3\Phi_g$ character excellent agreement with CASPT2 is obtained, whereas the states $a\,\Pi_g$ and $b\,\Delta_g$ which are predominantly $^3\Delta_g$ character are calculated too high by 2600–3100 cm^{-1}, conforming with the larger deviation found for the $^3\Delta_g$ state in Table II.

Finally, we would like to comment on the character and position of the luminescent state in both molecules. This state is shown in boldface in Tables VI and VII. As one can see, the predicted character of the luminescent state differs between different methods and also between the two mol-

ecules. For UO_2^{2+}, both DFT and CASPT2 agree that the luminescent state is $a\,\Delta_g$ originating primarily from a $\sigma_u^+ \rightarrow \phi_u$ ($^3\Phi_g$) excitation, whereas SOC-CI predicts a different state and configuration: $a\,\Pi_g$ with predominant $\sigma_u^+ \rightarrow \delta_u$ ($^3\Delta_g$) character. On the other hand, for $[UO_2Cl_4]^{2-}$, both CASPT2 and SOC-CI agree with experiment on $a\,E_g$ (corresponding to $a\,\Pi_g$ in $D_{\infty h}$) being the luminescent state, whereas DFT instead predicts a B_{2g} as the lowest excited state. The latter should, however, not be taken too strictly, given that the $a\,E_g$ state is found only 151 cm^{-1} higher in energy, and is, in fact, calculated lower by 276 cm^{-1} than the average of the two states $a\,B_{2g}$ and $a\,B_{1g}$ corresponding to $a\,\Delta_g$ (at 20 184 cm^{-1}) in $D_{\infty h}$. The fact that SOC-CI predicts the same luminescent state for both molecules, with an energy that differs by less than 400 cm^{-1}, is in line with the general trend of the SOC-CI results, indicating on the whole a very limited effect of the equatorial chlorines on the calculated excitation energies. More intriguing is the observation that both SAOP-TDDFT and CASPT2 instead do predict a different luminescent state and configuration, $a\,\Delta_g(\sigma_u^+ \rightarrow \phi_u)$, for the unknown spectrum of the bare UO_2^{2+} molecule than the $a\,E_g(\sigma_u^+ \rightarrow \delta_u)$ luminescent state observed experimentally in the well-known spectrum of $[UO_2Cl_4]^{2-}$ (and of other systems with a different equatorial surrounding, such as $[UO_2(NO_3)_3]^-$).[24] Furthermore, both methods predict a redshift of the luminescent state by about 2000 cm^{-1} in UO_2^{2+} as compared to $[UO_2Cl_4]^{2-}$, thus pointing to a distinct influence of the chlorine ligand field on the electronic spectrum of uranyl. At first sight this may seem unlikely, given that experimental data so far have rather indicated that the position of the bands between 20 000–30 000 cm^{-1} is quite indifferent to the nature of the equatorial field. However, these spectra have always been recorded in an equatorial surrounding that is saturated with ligands (be it four chorines, three nitrates, or a combination of ligands in solution spectra)[24,25,41–43] A recent CASPT2 investigation of the electronic spectra of uranyl chloride complexes in acetone[40] has confirmed that the excitation energies in such complexes indeed differ by no more than a few hundreds cm^{-1} between complexes with different numbers of equatorial chlorine/acetone ligands. The answer to the question whether the complete removal of all ligands from the equatorial plane would indeed introduce a shift in the electronic spectra predicted by the present SAOP-TDDFT or previous CASPT2 calculations can only come from an experimental spectrum of the bare uranyl ion.

IV. CONCLUSION

The lower part of the electronic spectra of UO_2^{2+} and $[UO_2Cl_4]^{2-}$ has been analyzed by means of a recently proposed relativistic TDDFT formalism, including the effects of spin-orbit coupling by means of the two-component zeroth-order regular approximation (ZORA). The results confirm the experimental interpretation and the results from previous theoretical calculations, that this part of the spectrum is built from excitations out of the HOMO σ_u^+ orbital into the nonbonding δ_u or ϕ_u uranyl orbitals. Scalar relativistic TDDFT calculations (i.e., without SOC) indicated that only the SAOP functional could give satisfactory excitation energies, while the results obtained with LDA, BP86, or even LB94 are far too low. The results of the two-component calculations (i.e., with SOC) were compared to experimental data (for $[UO_2Cl_4]^{2-}$) and to previous computational results obtained by either SOC-CI or CASSCF/CASPT2 (for UO_2^{2+} and $[UO_2Cl_4]^{2-}$). This comparison convincingly proves the quality of the DFT results. All calculated excitation energies and U–O distances and symmetric stretching frequencies closely correspond to both experiment (with average deviations of only 700 cm^{-1} for T_e and 28 cm^{-1} for ω_e) and to CASPT2, and are obviously superior to SOC-CI.

Even if some problems remain to be solved, such as the composition and the position of the σ_u^+ orbital in $[UO_2Cl_4]^{2-}$ and the appearance at too low energies of excitations out of the π_u orbital, we believe that this work presents a convincing first example of the strength of the two-component relativistic TDDFT approach recently proposed by Wang *et al.* for the research on spectroscopic properties of heavy element compounds.

ACKNOWLEDGMENTS

This investigation has been financially supported by grants from the Flemish Science Foundation (FWO) and from the Concerted Research Action of the Flemish Government (GOA).

[1] E. K. U. Gross, J. F. Dobson, M. Petersilka, in *Topics in Current Chemistry*, edited by R. F. Nalewajski (Springer, Heidelberg, 1996), Vol. 181, pp. 81–172.
[2] C. Jamorski, M. E. Casida, and D. R. Salahub, J. Chem. Phys. **104**, 5134 (1996).
[3] P. Pyykkö, Chem. Rev. (Washington, D.C.) **88**, 563 (1988).
[4] D. Toffoli, M. Stener, and P. Decleva, Phys. Rev. A **66**, 012501 (2002).
[5] J. Gao, W. Liu, B. Song, and C. Liu, J. Chem. Phys. **121**, 6658 (2004).
[6] F. Wang, T. Ziegler, E. van Lenthe, S. Van Gisbergen, and E. J. Baerends, J. Chem. Phys. **122**, 204103 (2005).
[7] E. van Lenthe, A. R. Ehlers, and E. J. Baerends, J. Chem. Phys. **110**, 8943 (1999).
[8] E. van Lenthe, E. J. Baerends, and J. G. Snijders, J. Chem. Phys. **99**, 4597 (1993).
[9] E. van Lenthe, E. J. Baerends, and J. G. Snijders, J. Chem. Phys. **101**, 9783 (1994).
[10] E. van Lenthe, J. G. Snijders, and E. J. Baerends, J. Chem. Phys. **105**, 6505 (1996).
[11] E. van Lenthe, R. van Leeuwen, J. G. Snijders, and E. J. Baerends, Int. J. Quantum Chem. **57**, 281 (1996).
[12] H. Eschrig and V. D. P. Servedio, J. Comput. Chem. **20**, 23 (1999).
[13] C. van Wüllen, J. Comput. Chem. **23**, 779 (2002).
[14] F. Wang and W. Liu, J. Chin. Chem. Soc. (Taipei) **50**, 597 (2003).
[15] G. te Velde, F. M. Bickelhaupt, E. J. Baerends, C. Fonseca Guerra, S. J. A. van Gisbergen, J. G. Snijders, and T. Ziegler, J. Comput. Chem. **22**, 931 (2001).
[16] S. J. A. van Gisbergen, J. G. Snijders, and E. J. Baerends, Comput. Phys. Commun. **118**, 119 (1999).
[17] Amsterdam Density Functional (ADF), SCM, Theoretical Chemistry, Vrije Universiteit, Amsterdam, The Netherlands, http://www.scm.com.
[18] F. Wang and T. Ziegler, J. Chem. Phys. **123**, 194102 (2005).
[19] K. Tatsumi and R. Hoffmann, Inorg. Chem. **19**, 2656 (1980).
[20] C. K. Jørgensen and R. Reisfeld, Struct. Bonding (Berlin) **50**, 121 (1982).
[21] R. L. DeKock, E. J. Baerends, P. M. Boerrigter, and J. G. Snijders, Chem. Phys. Lett. **105**, 308 (1984).
[22] N. Kaltsoyannis, Inorg. Chem. **39**, 6009 (2000).
[23] N. Kaltsoyannis, Chem. Soc. Rev. **32**, 9 (2003).
[24] R. G. Denning, Struct. Bonding (Berlin) **79**, 215 (1992).

[25] T. J. Barker, R. G. Denning, and J. R. G. Thorne, Inorg. Chem. **26**, 1721 (1987).
[26] C. Görller-Walrand and L. G. Vanquickenborne, J. Chem. Phys. **57**, 1436 (1972).
[27] C. Görller-Walrand and L. G. Vanquickenborne, J. Chem. Phys. **54**, 4178 (1971).
[28] Z. Zhang and R. M. Pitzer, J. Phys. Chem. A **103**, 6880 (1999).
[29] S. Matsika and R. M. Pitzer, J. Phys. Chem. A **105**, 637 (2001).
[30] K. Pierloot and E. van Besien, J. Chem. Phys. **123**, 204309 (2005).
[31] S. Vosko, L. Wilk, and M. Nusair, Can. J. Phys. **58**, 1200 (1980).
[32] A. D. Becke, Phys. Rev. A **38**, 3098 (1988).
[33] J. P. Perdew, Phys. Rev. B **33**, 8822 (1986).
[34] R. van Leeuwen and E. Baerends, Phys. Rev. A **49**, 2421 (1994).
[35] P. R. T. Schipper, O. V. Gritsenko, S. J. A. van Gisbergen, and E. J. Baerends, J. Chem. Phys. **112**, 1344 (2000).
[36] J. P. Perdew, J. A. Chevary, S. H. Vosko, K. A. Jackson, M. R. Pederson, D. J. Singh, and C. Fiolhais, Phys. Rev. B **46**, 6671 (1992).
[37] E. van Lenthe and E. J. Baerends, J. Comput. Chem. **24**, 1142 (2003).
[38] A. Rosa, G. Ricciardi, O. Gritsenko, and E. J. Baerends, Struct. Bonding (Berlin) **112**, 49 (2004).
[39] R. K. Szilagyi, M. Metz, and E. I. Solomon, J. Phys. Chem. A **106**, 2994 (2002).
[40] E. van Besien and K. Pierloot, Phys. Chem. Chem. Phys. **8**, 4311 (2006).
[41] S. De Houwer and C. Görller-Walrand, J. Alloys Compd. **323**, 683 (2001).
[42] C. Görller-Walrand, S. De Houwer, L. Fluyt, and K. Binnemans, Phys. Chem. Chem. Phys. **6**, 3292 (2004).
[43] M. Garcia-Hernandez, C. Willnauer, S. Kruger, L. V. Moskaleva, and R. N. Inorg, Inorg. Chem. **45**, 1356 (2006).